AEROELASTIC STABILITY OF A COMPOSITE WING BOX WITH UNCERTAINTIES IN MATERIAL PROPERTIES

C. Scarth[a*], J. E. Cooper[a], G. H. C. Silva[b]

[a] *Department of Aerospace Engineering, University of Bristol, Queen's Building, University Walk, Bristol, BS8 1TR, United Kingdom*
[b] *Embraer S.A., Av. Brigadeiro Faria Lima, 2170, 12227-901, São José dos Campos, São Paulo, Brazil*
** cs5938@bristol.ac.uk*

Abstract
An approach is presented for modelling the effects of uncertainty in modulus and ply orientation upon the aeroelastic stability of a composite wing box. The wing box is modelled as a thin-walled beam which incorporates the effects of transverse shear. Uncertainties are propagated through the model using Polynomial Chaos Expansion, with coefficients determined using Stochastic Projection and Smolyak sparse grid quadrature. Laminate stiffness terms are used as input variables in order to avoid the curse of dimensionality. An order of magnitude reduction in model runs is achieved for the majority of example laminates; however, the approach gives poor results in the region of response discontinuities.

1. Introduction

Composite materials are being used to increasing degree in aerospace structures due to benefits such as high specific strength and stiffness, and anisotropic behaviour which may be exploited to tailor the properties of the structure. A large amount of work has been undertaken since the 1980s in the field of aeroelastic tailoring [1-4]. This has sought to exploit anisotropy through selection of composite stacking sequences to achieve minimum-weight designs for aeroelastic design cases such as divergence [1] and flutter [2-3] as well as gust and manoeuvre loads [4], while adhering to efficient aerodynamic design and loading constraints.

In reality all processes are subject to variability and a need for robust processes which directly incorporate uncertainties into design has been identified [5]. Furthermore, composite materials use complex manufacturing processes which can introduce uncertainty from a number of sources including material non-homogeneity, fibre misalignment and waviness [6].

The most straightforward uncertainty quantification technique is Monte Carlo Simulation (MCS). This requires a prohibitively large computational effort, and techniques such as Polynomial Chaos Expansion (PCE) can be more efficient. PCE was first introduced in [7] and subsequently developed as part of the Stochastic Finite Element method [8]. Methods such as stochastic projection [9] seek to apply the expansions in a 'non-intrusive' fashion such that they may be used with any 'black-box' deterministic model. PCE is limited by the 'curse of dimensionality', whereby the size of the model grows substantially with the number of inputs; a number of methods have been developed to combat this, including the use of sparse grid quadrature [10] and adaptive algorithms for tailoring the size of the expansion [11].

Much of the existing work which models the effects of composite material property uncertainty upon aeroelastic stability uses computationally expensive MCS, or techniques which give limited information on the full distribution. For example, the perturbation method is used in [12] to model supersonic flutter of a composite plate and in [13] to model flutter of a composite beam. The body of work which uses more efficient techniques such as PCE has largely used simplified structural behavior or has modelled aerodynamic uncertainties. A number of pitch and plunge aerofoil models with uncertain spring stiffness coefficients are reviewed in [5], and [14] models the response of a flat plate with uncertain aerodynamic load.

Polynomial Chaos Expansion was used in [15] to model aeroelastic stability of composite plate wings with uncertain ply orientation; this was limited to the design space of six ply symmetric laminates. The authors generalised this approach to any symmetric laminate in [16], by using 'lamination parameters' as input random variables. This paper aims to build upon previous work by using PCE to model material property uncertainty, in particular ply orientation uncertainty, in more realistic aerospace structures. A wing box model is introduced in section 2 and section 3 provides an overview of PCE using sparse grid quadrature. Section 4 presents results of application of this method to the wing box with uncertainty in modulus and ply orientation introduced to the top and bottom flanges.

2. Wing-Box Model

2.1. Beam Model

A thin-walled beam similar to those in [17] and [18] is used to model a composite wing box. Two coordinate systems are used; a global wing and a local laminate coordinate system, both of which are shown in Figure 1.

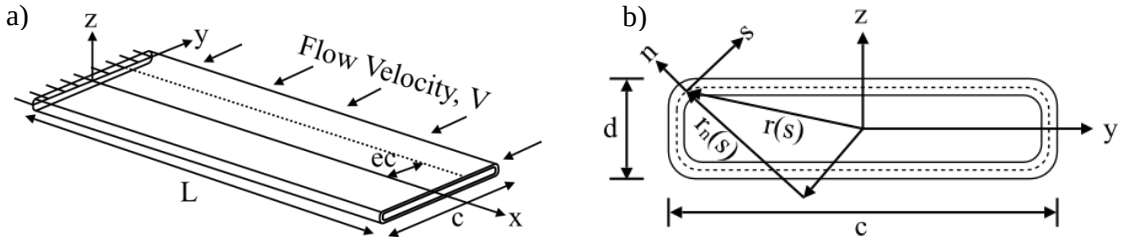

Figure 1. Global (a) and Local (b) Coordinate Systems used in the Beam Model

Kinematic relationships reduce displacements of the three-dimensional structure to a one dimensional dependence upon *x*:

$$u(x,y,z) = u_0(x) - \theta_z(x)y(s) + \theta_y(x)z(s) \tag{1}$$

$$v(x,y,z) = v_0(x) - \phi(x)z(s) \tag{2}$$

$$w(x,y,z) = w_0(x) + \phi(x)y(s) \tag{3}$$

Behaviour of the model is described by six kinematic variables; u_0, v_0 and w_0 denote displacement of the reference axis in the x, y and z directions, and ϕ, θ_y and θ_z denote rotation of the reference axis about the x, y and z axes. Using (1), local axial strain is given by:

$$\varepsilon_{xx} = u_0' - \theta_z' y + \theta_y' z \tag{4}$$

where a primed variable denotes differentiation with respect to x. Shear flow due to torsion is assumed as St Venant's solution, weighted by laminate shear stiffness A_{66} to account for different stacking sequences around the section. Introducing the continuity requirement, $\oint \frac{\partial u}{\partial s} ds = 0$, and using (1-3), the shear strain is therefore expressed as:

$$\gamma_{xs} = \frac{dy}{ds}(v_0' - \theta_z) + \frac{dz}{ds}\left(w_0' + \theta_y\right) + \frac{2A_C}{A_{66}\oint \frac{ds}{A_{66}}}\phi' \tag{5}$$

where A_c is the area enclosed by the section. Since only global deformations are of interest and the design is restricted to symmetric laminates, it is assumed that behavior is governed solely by membrane properties. In-plane stress resultants are related to in-plane strains by:

$$\{N\} = [A]\{\varepsilon\} \tag{6}$$

where A is the laminate membrane stiffness. Assuming zero stress resultant in the tangential direction, (6) may be re-written with dependence only upon the x coordinate:

$$\begin{Bmatrix} N_x \\ N_{xs} \end{Bmatrix} = \begin{bmatrix} A_{11} - \frac{A_{12}^2}{A_{22}} & A_{16} - \frac{A_{12}A_{16}}{A_{22}} \\ A_{16} - \frac{A_{12}A_{16}}{A_{22}} & A_{66} - \frac{A_{16}^2}{A_{22}} \end{bmatrix} \begin{Bmatrix} \varepsilon_{xx} \\ \gamma_{xs} \end{Bmatrix} \tag{7}$$

Henceforth, the matrix in (7) is referred to as the 'modified laminate stiffness' or $\hat{A}$.

2.2. Aeroelastic Stability

Aeroelastic response of the beam is modelled using Rayleigh Ritz coupled with modified unsteady strip theory [19]. In this approach polynomial shape functions are assumed for each kinematic variable in order to approximate energy terms. Strain energy is given as:

$$U = \frac{1}{2}\int_0^L \oint \{\boldsymbol{\varepsilon}\}^T \left[\hat{A}\right] \{\boldsymbol{\varepsilon}\} ds dx \tag{8}$$

where {ε} is given by (4) and (5). Kinetic energy is given as:

$$T = \frac{1}{2}\int_0^L \oint \int_{-\frac{t}{2}}^{\frac{t}{2}} \rho \{\dot{\boldsymbol{u}}\}^T \{\dot{\boldsymbol{u}}\} dn\, ds\, dx \tag{9}$$

where $\{\mathbf{u}\} = \{u, v, w\}^T$ is the beam displacement vector given by (1-3), ρ is the density and t the thickness. Lift and pitching moment are applied to infinitesimal strips at the quarter chord and integrated over the length of the beam. The loads applied to each strip are given by:

$$dL = \frac{1}{2}\rho_a V^2 c a_w \left(\phi - \frac{\dot{w}_0}{V}\right) dx \tag{10}$$

$$dM = \frac{1}{2}\rho_a V^2 c^2 \left(e a_w \left(\phi - \frac{\dot{w}_0}{V}\right) + M_{\dot{\theta}} \frac{\dot{\phi} c}{4V}\right) dx \tag{11}$$

where ρ_a and V denote the air density and velocity, c the chord length, e the eccentricity between the quarter chord and reference axis, and a_w the effective lift curve slope. A simplified analysis whereby the unsteady aerodynamic derivative $M_{\dot{\theta}}$ is assumed to be constant with frequency is used. Work done by the applied load is given by:

$$\delta W = \int_0^L (dL\delta w + dM\delta\theta)dx \tag{12}$$

Neglecting dissipative energy, Lagrange's Equation may be applied as:

$$\frac{d}{dt}\left(\frac{\partial T}{\partial \dot{\boldsymbol{q}}}\right) - \frac{\partial T}{\partial \boldsymbol{q}} + \frac{\partial U}{\partial \boldsymbol{q}} = \frac{\partial(\delta W)}{\partial(\delta \boldsymbol{q})} \tag{13}$$

where $\boldsymbol{q}$ are the generalised displacements. Application of (13) gives equation of motion as:

$$[A]\{\ddot{\boldsymbol{q}}\} + \rho_a V[B]\{\dot{\boldsymbol{q}}\} + (\rho_a V^2[C] + [E])\{\boldsymbol{q}\} = \{\boldsymbol{0}\} \tag{14}$$

where [A] is the mass matrix, [B] and [C] are the aerodynamic damping and stiffness matrices, and [E] is the structural stiffness matrix. Equation (14) can be solved as an eigenvalue problem. Instability occurs when the real part of one of the eigenvalues becomes positive; this instability is flutter if the imaginary part is non-zero and divergence otherwise.

Bend-twist coupling may be achieved in the present beam model through using opposite stacking sequences on opposing flanges. Figure 2 shows example plots of eigenvalues with increasing flow velocity for two examples with opposite coupling properties.

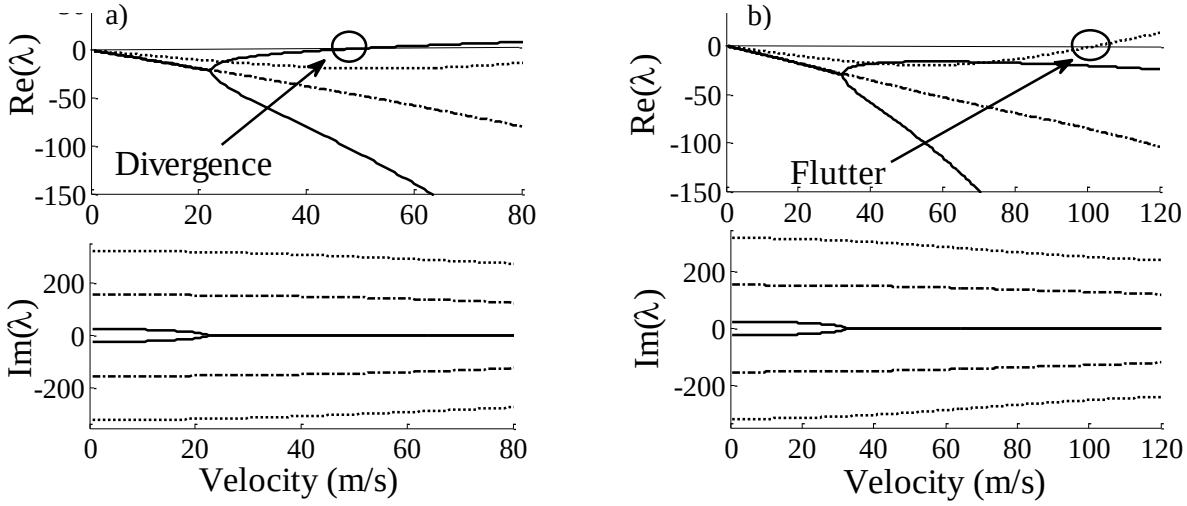

Figure 2. Plots of Real and Imaginary parts of Eigenvalues with Speed for a beam with $[\pm 45]_S$ webs and: a) Top Flange: $[-45]_4$, Bottom Flange: $[45]_4$ b) Top Flange $[45]_4$, Bottom Flange $[-45]_8$.

3. Uncertainty Quantification

3.1. Polynomial Chaos Expansion using Smolyak Sparse Grids

Polynomial Chaos Expansion (PCE) is used to propagate uncertainty through the aeroelastic model. Any second-order random process may be written as [8]:

$$\begin{aligned} X(\omega) = \alpha_0\Gamma_0 + \sum_{i_1=1}^{\infty}\alpha_{i_1}\Gamma_1\left(\xi_{i_1}(\omega)\right) + \sum_{i_1=1}^{\infty}\sum_{i_2=1}^{i_1}\alpha_{i_1 i_2}\Gamma_2\left(\xi_{i_1}(\omega),\xi_{i_2}(\omega)\right) \\ + \sum_{i_1=1}^{\infty}\sum_{i_2=1}^{i_1}\sum_{i_3=1}^{i_2}\alpha_{i_1 i_2 i_3}\Gamma_3\left(\xi_{i_1}(\omega),\xi_{i_2}(\omega),\xi_{i_3}(\omega)\right) + \cdots \end{aligned} \tag{15}$$

where ω a random event, $\{\xi_{i1}(\omega)\}_1^{\infty}$ is a set of independent random variables, $\Gamma_p\left(\xi_{i1}(\omega),\ldots,\xi_{ip}(\omega)\right)$ is the polynomials chaos of order p, and $\alpha_{i1,\ldots,ip}$ are the expansion coefficients. In practice (15) is truncated, and for notational clarity rewritten:

$$X(\omega) = \sum_{i=0}^{\mathrm{P}} \beta_i \, \psi_i(\boldsymbol{\xi}(\omega)) \tag{16}$$

Equation (16) is a complete polynomial basis which is orthogonal with respect to the Probability Density Function (PDF) of the input variables, and therefore guarantees exponential convergence with increasing expansion order. For example, Hermite Polynomials form a basis which is orthogonal with respect to standard Gaussian input random variables.

In order to determine the unknown expansion coefficients, model outputs are projected against each basis polynomial using the inner product and orthogonality is exploited [9]:

$$\beta_i = \frac{\langle R, \psi_i \rangle}{\langle \psi_i^2 \rangle} = \frac{1}{\langle \psi_i^2 \rangle} \int_{\Omega} R \psi_i W(\boldsymbol{\xi}) d\boldsymbol{\xi} \tag{17}$$

Evaluation of (17) requires multidimensional integration of outputs (R) across the support (Ω) of the input PDF ($W(\boldsymbol{\xi})$). Univariate integrals may be approximated using quadrature rules:

$$\mathcal{U}^i(f)(\xi) = \sum_{j=1}^{m_i} f\left(\xi_j^i\right) w_j^i \tag{18}$$

where ξ_j^i are quadrature points, w_j weights, and m_i the number of points. Quadrature rules should be selected according the input distribution, for example, Gauss-Hermite Quadrature for Gaussian inputs. In order to combat the curse of dimensionality, Smolyak sparse grids are used to efficiently generate multivariate quadrature rules from the univariate rules [14]:

$$\mathcal{A}(w, n) = \sum_{w+1 \le |\boldsymbol{i}| \le w+n} (-1)^{w+n-|\boldsymbol{i}|} \binom{n-1}{w+n-|\boldsymbol{i}|} \cdot \left(\mathcal{U}^{i_1} \otimes \ldots \otimes \mathcal{U}^{i_n}\right) \tag{19}$$

where w defines the precision of the quadrature, n is the number of dimensions, and $\boldsymbol{i} = (i_1, \ldots, i_n)$ is a multi-index. (19) is a linear combination of tensor products of univariate quadrature rules, which only uses products that result in a relatively low number of points.

Polynomial Chaos Expansion requires that input random variables are statistically independent. Dependent random variables of arbitrary distribution may be transformed onto independent uniform variables using the Rosenblatt transformation [20]:

$$\begin{aligned} y_1 &= F_1(x_1) \\ y_2 &= F_2(x_2|x_1) \\ &\vdots \\ y_n &= F_n(x_n|x_{n-1}, \ldots, x_1) \end{aligned} \tag{20}$$

4. Results

The above techniques have been used to determine the critical aeroelastic instability speed with uncertainty in different inputs, using the geometry and average properties in Table 1.

Length (m)	Chord (m)	Depth (m)	E_{11} (GPa)	E_{22} (GPa)	G_{12} (GPa)	ν_{12}	ρ (kg/m^3)	Ply Thickness (mm)
4	0.8	0.08	140	10	5	0.3	1600	0.125

Table 1. Dimensions and average material properties used in the case studies

To demonstrate a straightforward application of Polynomial Chaos Expansion, uncertainty is introduced into E_{11}, E_{22} and G_{12} in the top and bottom flanges. Uncertainty is neglected in the webs due to their relatively small size, and the stacking sequence of all components is $[0\ 90\ \pm 45]_S$. The variables are modelled as Gaussian, with mean given by Table 1 and coefficient of

variation of 0.1. Figure 3 shows convergence of the PCE with different expansion order compared to results from a Monte Carlo Simulation using 7,500 samples. It can be seen that third order PCE acceptably models both the peak and tails. This calculation required 73 model evaluations, offering an improvement in efficiency of two orders of magnitude.

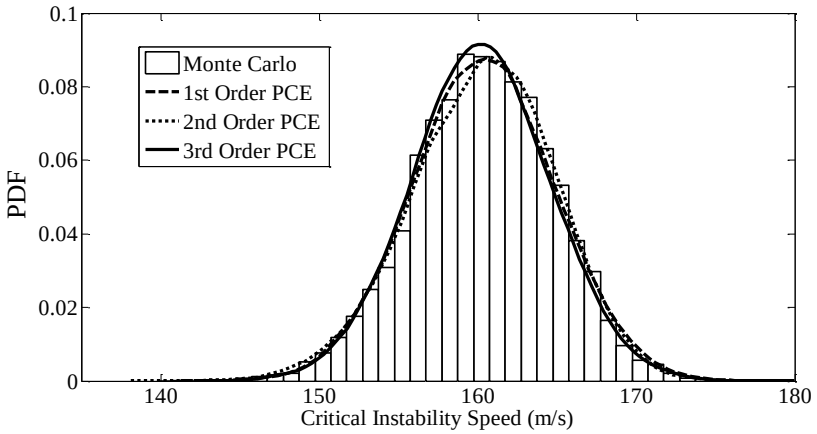

Figure 3. Convergence of Polynomial Chaos Expansion using Polynomials of ascending order for a beam with all components having a $[0, 90, \pm 45]_S$ stacking sequence

Uncertainty is now introduced to the ply orientations in the top and bottom flanges, considerably increasing the input dimension. Error in each ply is modelled as Gaussian with zero mean and standard deviation of 5 degrees, and uncertainty in E_{11}, E_{12} and G_{12} is modelled as above. The dimension of the PCE is reduced to six by using the modified A matrix terms from (7) as input random variables. The PDFs of these terms are determined using MCS and transformed onto standard Gaussian distributions using the Rosenblatt Transformation. Details of results for a number of example configurations are shown in Table 2, with example PDFs shown in Figures 4 and 5.

Configuration		PCE Order	Model Runs
All Components:	$[0]_8$	4	257
All Components:	$[90]_8$	2	13
All Components:	$[0_2\ 90_2]_S$	3	73
All Components:	$[0\ 90\ \pm 45]_S$	1	13
All Components:	$[(\pm 45)_2]_S$	> 6	> 2021
Top Flange: Bottom Flange:	$[45]_8$ $[-45]_8$	3	73
Top Flange: Bottom Flange:	$[-45]_8$ $[45]_8$	4	257

Table 2. Required expansion order and model runs for each of the example laminates

For most of the examples, 3rd or 4th order PCE requiring to 73 and 257 model runs respectively was sufficient, corresponding to a factor of 30 reduction compared to Monte Carlo. Due to the relative expense of the 4th order PCE, it is noted that the sparse grid method loses its benefit for higher expansion order. Figure 5 shows bi-modal behavior, which can be attributed to a mode-switch in the region spanned by the output PDF [16]. Very high order PCE is required to model this behaviour; convergence of the PCE is consequentially shown up to 6th order in Figure 5, at which point the analysis was halted due to the computational effort approaching that of MCS.

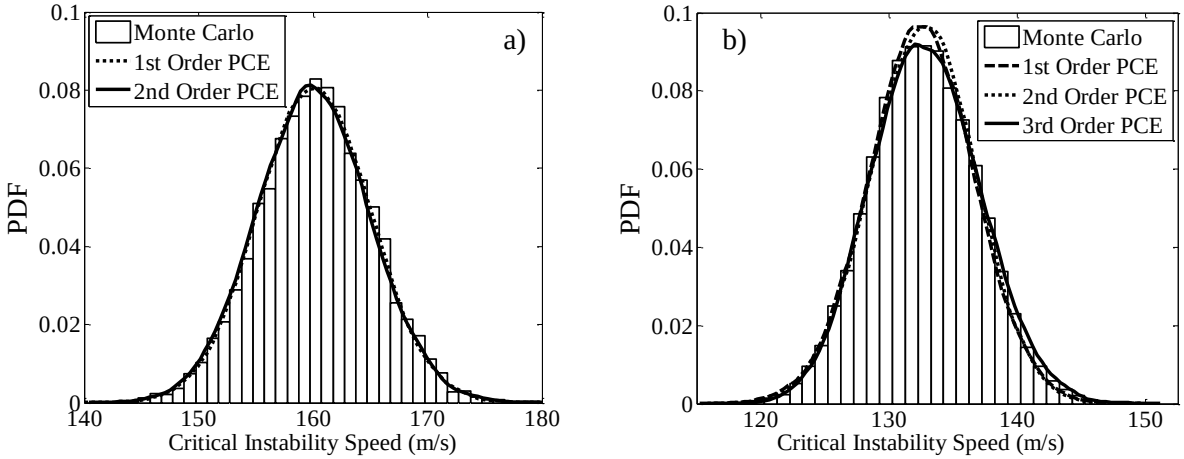

Figure 4. Convergence of PCE using Polynomials of ascending order for a beam with a) all components having a $[0, 90, \pm 45]_S$ stacking sequence, b) Top Flange $[45]_8$, bottom Flange $[-45]_8$ and Webs $[\pm 45]_S$

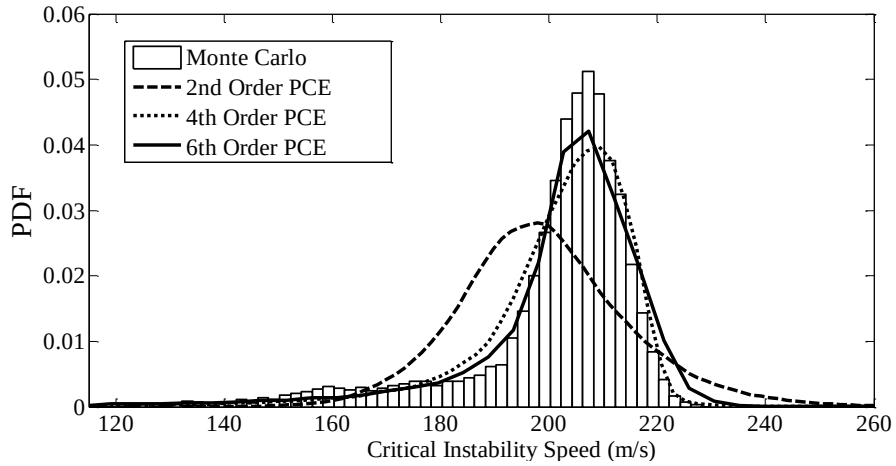

Figure 5. Convergence of PCE using Polynomials of ascending order for a beam with all components having the stacking sequence $[\pm 45]_S$. Example of Bi-modal behaviour

5. Conclusions

An approach has been presented for modelling aeroelastic stability of a composite wing box with uncertainty in modulus and ply orientation. Polynomial Chaos Expansion using sparse grid quadrature and modified laminate stiffness input variables were used to avoid the 'Curse of Dimensionality', while building upon the work in [16] through modelling a more realistic structure. The following observations have been made:

- In the majority of examples, 3rd or 4th order PCE proved sufficient, leading to at least a factor of 30 reduction in aeroelastic model runs compared to the baseline Monte Carlo.
- Sparse-grid quadrature is efficient for high-dimension inputs in low order expansions, however, this benefit is insufficient for higher order PCE. It is suggested that 'tailored' PCE using adaptive algorithms [11] could be used to increase the dimension further.
- Very high order PCE is required to model the bi-modal behavior associated with a mode-switch in aeroelastic response. It is suggested that the approach developed in [16] be adapted for use with the quadrature method, or a piece-wise PCE employed.

Acknowledgements

The authors would like to recognise the support of the EPSRC and Embraer S.A.

References

[1] T. A. Weisshaar. Aeroelastic Tailoring of Forward Swept Composite Wings. *J. Aircraft*, 18(8):669-676, 1981.
[2] T. A. Weisshaar, R. J. Ryan. Control of Aeroelastic Instabilities through Stiffness Cross-Coupling. *J. Aircraft*, 23(2):148-155, 1986.
[3] M. Kameyama, H. Fukunaga. Optimum Design of Composite Plate Wings for Aeroelastic Characteristics using Lamination Parameters. *Comput Struct*, 85(3-4):213-224, 2007.
[4] C. L. Pettit, R. V. Grandhi. Optimization of a Wing Structure for Gust Response and Aileron Effectiveness. *J. Aircraft*, 40(6):1185-1191, 2003.
[5] C. L. Pettit. Uncertainty Quantification in Aeroelasticity: Recent Results and Research Challenges. *J. Aircraft*, 41(5):1217-1229, 2004.
[6] K. Potter, B. Khan, M. R. Wisnom, T. Bell, J. Stevens. Variability, Fibre Waviness and Misalignment in the Determination of the Properties of Composite Materials and Structures. *Composites: Part A*, 39(9):1343-1354, 2008.
[7] N.Wiener. The Homogeneous Chaos. *Amer. J. Math.*, 60(4):897-936, 1938.
[8] R. G. Ghanem, P. G. Spanos. *Stochastic Finite Elements: A Spectral Approach.* Springer-Verlag, New York, 1991.
[9] O.P. Le Maître, M. T. Reagan, H. N. Najm, R. G. Ghanem, O. M. Knio. A Stochastic Projection Method for Fluid Flow: II. Random Process. J *Comput Phys* 181(1):9-44,2002.
[10] M. S. Eldred, J. Burkardt. Comparison of Non-Intrusive Polynomial Chaos and Stochastic Collocation Methods for Uncertainty Quantification. In *47th AIAA Aerospace Sciences Meeting Including the New Horizons Forum and Aerospace Exposition*, Orlando, Florida, 2009.
[11] G. Blatman, B. Sudret. An Adaptive Algorithm to Build up Sparse Polynomial Chaos Expansions for Stochastic Finite Element Analysis. *Probab. Eng. Mech.* 25(2):183-197, 2010.
[12] D. G. Liaw, H. T. Y. Yang. Reliability of Uncertain Laminated Shells due to Buckling and Supersonic Flutter. *AIAA J*, 29(10):1698-1708, 1993.
[13] S. C. Castravete, R. A. Ibrahim. Effect of Stiffness Uncertainties on Flutter of a Cantilever Wing. *J. Aircraft*, 46(4):925-935, 2008.
[14] L. Bruno, C. Canuto, D. Fransos. Stochastic Aerodynamics and Aeroelasticity of a Flat Plate via Generalized Polynomial Chaos. *J. Fluids Struct*, 25(7):1158-1176, 2009.
[15] A. Manan, J. E. Cooper. Design of Composite Wings Including Uncertainties: A Probabilistic Approach. *J. Aircraft*, 46(2):601-607, 2009.
[16] C. Scarth, J. E. Cooper, P. M. Weaver, G. H. C. Silva. Uncertainty Quantification in Aeroelastic Composite Structures using Lamination Parameters. In *The International Forum for Aeroelasticity and Structural Dynamics (IFASD)*, Bristol, UK, 2013.
[17] R. Chandra, I. Chopra. Structural Response of Composite Beams and Blades with Elastic Couplings. *Compos. Eng*, 2(5-7):347-374, 1992.
[18] L. Librescu, O. Song. On the Static Aeroelastic Tailoring of Composite Aircraft Swept Wings Modelled as Thin-Walled Beam Structures. *Compos. Eng*, 2(5-7):497-512, 1992.
[19] J. R. Wright, J. E. Cooper. *Introduction to Aircraft Aeroelasticity and Loads*. Wiley, New York, 2007.
[20] M. Rosenblatt. Remarks on a Multivariate Transformation. *Ann. Math. Stat.* 23(3):470-472, 1952.